

Global Mapping of the Whole-Brain Network Underlining Binocular Rivalry

Masanori Shimono^{1,2} and Kazuhisa Niki³

Abstract

We investigated how the structure of the brain network relates to the stability of perceptual alternation in binocular rivalry. Historically, binocular rivalry has provided important new insights to our understandings in neuroscience. Although various relationships between the local regions of the human brain structure and perceptual switching phenomena have been shown in previous researches, the global organization of the human brain structural network relating to this phenomenon has not yet been addressed. To approach this issue, we reconstructed fiber-tract bundles using diffusion tensor imaging and then evaluated the correlations between the speeds of perceptual alternation and fractional anisotropy (FA) values in each fiber-tract bundle integrating among 84 brain regions. The resulting comparison revealed that the distribution of the global organization of the structural brain network showed positive or negative correlations between the speeds of perceptual alternation and the FA values. First, the connections between the subcortical regions stably were negatively correlated. Second, the connections between the cortical regions mainly showed positive correlations. Third, almost all other cortical connections that showed negative correlations were located in one central cluster of the subcortical connections. This contrast between the contribution of the cortical regions to destabilization and the contribution of the subcortical regions to stabilization of perceptual alternation provides important information as to how the global architecture of the brain structural network supports the phenomenon of binocular rivalry.

Key words: cortex; global architecture, human brain network; diffusion tensor imaging; perceptual alternation; subcortex

Introduction

BINOCULAR RIVALRY HAS an ancient and storied history in cognitive psychology (Levelt, 1965; Sherrington, 1906; Wade, 1998; Wheatstone, 1838). In binocular rivalry experiments, the right and left eyes are presented with different images simultaneously at the same retinal position. From these two physically constant visual images, participants tend to perceive only one of two images. This unique perception alternates between two images spontaneously in a phenomenon called perceptual alternation.

Before recording technologies were used to study this phenomenon, some researchers hypothesized that a perceptual alternation happened when activity of the neuron pool corresponding to a dominant perception decayed (Grossberg, 1987; Hock *et al.*, 1997; Kohler, 1940). Further, for several decades, psychophysical researches questioned where the competing neuron pool is located in the brain. Specifically, they believed that either

low-level visual regions, such as the primary visual cortex or lateral geniculate nucleus (LGN), or high-level visual regions, such as the extrastriate visual regions, may be the center of competition (Blake, 1989; Kovacs, *et al.*, 1996; Lehky, 1998; Logothetis *et al.*, 1996; Matsuoka, 1984; Sugie, 1982).

An example supporting the low-level visual processing hypothesis is the traveling wave, a phenomenon of visual alternation starting from partial patches in the visual field expanding to the full image. In the traveling wave, the interaction between visual information occurred along the retinotopically adjacent visual fields, and retinotopic maps exist on the early visual field more clearly (Wilson *et al.*, 2001).

An example supporting this high-level visual processing hypothesis is the demonstration that when two visual stimuli are rapidly alternated between the two eyes, the temporal dynamics of perceptual alternation are similar as when the stimuli were not alternated (Logothetis *et al.*, 1996). This hypothesis is also supported by evidence showing that

¹Department of Physics, Indiana University, Bloomington, Indiana.

²Graduate School of Education, University of Tokyo, Tokyo, Japan.

³Human Technology Research Institute, National Institute of Advanced Industrial Science and Technology, Tsukuba, Japan.

intraocular interactions exist (Kovacs *et al.*, 1996). Psychophysical experiments in monkeys and functional magnetic resonance-imaging (fMRI) studies in humans demonstrated that the highest correlation of brain activity occurs within the extrastriate visual cortex (Leopold and Logothetis, 1996; Logothetis and Schall, 1989; Tong *et al.*, 1998).

More-detailed observations of these same psychophysical experiments showed the replication and limitations of both hypotheses (Lee and Blake, 1999, 2004). Recently, the relationship between the neural activity in V1 and the LGN has also been observed (Haynes *et al.*, 2005; Lee *et al.*, 2007; Lehky, 1988; Winderlich *et al.*, 2005).

Whether low-level regions or high-level regions are the center of competition underlying binocular rivalry is still in debate, and the mutual combinational theory has also been proposed, which is based on a hierarchical model with sequential competitions in both the low-level and in the high-level layers of the visual cortex. Based on this theory, both layers would contribute to the perceptual alternation phenomenon, even though their properties are very different (Blake and Logothetis, 2002; Nguyen *et al.*, 2001; Ooi and He, 2003; Tong *et al.*, 2006).

In a wider view, several fMRI studies have found that the right prefrontal region and the parietal region become active at the times when perceptual alternations happened (Kleinschmidt *et al.*, 1998; Knapen *et al.*, 2011; Lumer and Friston, 1998; Sterzer and Kleinschmidt, 2007). In studies of volume-based morphometry and diffusion tensor imaging (DTI), using the parietal cortex structure, it is possible to predict the differences in stability of perceptual alternation (Kanai *et al.*, 2010a). For example, an fMRI study showed that the parietal and frontal regions play a central role in intentional stabilization and alternation of perceptions (Shimono *et al.*, 2011a; Sterzer and Kleinschmidt, 2007). A study of patients with brain injury showed that the prefrontal cortex is important for the acceleration of perceptual alternation (Windmann *et al.*, 2006). Although many studies have reported that various brain regions, such as the primary visual cortex, extrastriate visual cortex, parietal cortex, frontal cortex, and thalamus, contribute to different aspects of the perceptual alternation phenomenon, the whole-brain interactions are not fully understood.

Based on these previous findings, we asked what structural brain networks support the dynamic interactions between various brain regions. In particular, previous studies did not examine the global organization of the structural brain network. The effectiveness of this network-based approach has previously been demonstrated (Bullmore and Sporns, 2009; Sporns *et al.*, 2005) in characterizing the default-mode network of the general global brain architecture (Hagmann *et al.*, 2007, 2008), and in the pathognomonic status and specific cognitive ability (Hanggi, *et al.*, 2011; Lynall *et al.*, 2010). Although the interaction among many brain regions is reported frequently in studies of synchronization of EEG signals recorded from head surfaces, there has been no study reporting direct comparisons between anatomical networks in perceptual behavior (Doesburg *et al.*, 2005, 2009; Hipp *et al.*, 2011; Struber *et al.*, 2000; Varela *et al.*, 2001).

In this study, we recorded both behavioral data in binocular rivalry experiments and DTI data from participants. Then, we extracted the important fiber-tract bundles based on whether mean fractional anisotropy (FA) values show significant positive or negative correlation with the alternation speeds. FA value is thought to reflect the information transmission efficiency

on each fiber tract (Head *et al.*, 2004; Klingberg *et al.*, 2000; Pfefferbaum *et al.*, 2002). The spatial mapping of fiber-tract bundles having negative or positive correlations revealed that global modules such as groups of the cortical or subcortical regions are responsible for stability of perception in binocular rivalry. Therefore, the significant positive or negative correlations of fiber-tract bundles indicate the high information transmission efficiency relating to acceleration or deceleration of perceptual alternation.

Materials and Methods

Participants

Seventeen healthy, right-handed volunteers (aged from 20 to 29 years; 10 men and 7 women) were recruited for the experiment. Participants did not have a history of neurological or psychiatric disorders. All participants had normal or corrected-to-normal vision. All procedures were approved by the AIST MRI safety and ethics committee, and informed consent was obtained from all participants before the experiment was conducted. We performed DTI recordings and the psychophysical experiments in the MRI room on the first day. Approximately 3 weeks later, 12 of the participants participated in the psychophysical experiment to evaluate the stability of speeds of the perceptual alternation.

General scheme of data processing

Analysis consisted of four procedures (Fig. 1). First, we performed preprocessing of diffusion-weighted images to reduce noise and coregistration, and calculated the three-dimensional maps of FA values. Second, we segmented the brain into 68 cortical regions and 16 subcortical regions. Third, we reconstructed the fiber tracts connecting among these regions by tracking the vector map of FA values. We then defined the weight of each fiber-tract bundle based on the mean FA value of all voxels in each of the fiber-tract bundle. Fourth, we compared the architecture of reconstructed networks with the results of psychophysical experiments.

MRI acquisition

All scanning was performed on a 3.0 T MRI Scanner (3T Signa LX; General Electric Medical Systems, Milwaukee, MN) equipped with an echo-planar imaging (EPI) capability and a standard head coil. During scanning, subjects remained supine with their heads immobilized with cushioned supports, wearing earplugs to weaken the MRI-gradient noise.

Diffusion-weighted imaging was acquired using a single-shot EPI spin-echo (EPI-SE) pulse sequence with the following parameters: 51 axial slices, TR 16 sec, TE 8.83 milliseconds, number of excitations (NEX) 1, FOV 320 mm (covering the whole cerebrum), acquisition matrix 128×128, reconstructed to 256×256, and 2.5-mm slice thickness using no interslice gap. Diffusion-sensitizing gradients were applied along 33 directions with a diffusion sensitivity of $b=0$ and 1000 s/mm². The studies also included the fast spin-echo (FSE) T2-weighted (TR: 500, TE: 9.8, FA: 90, NEX: 1) and gradient Echo T1-weighted (TR: 1.07, FA: 0.3, FA: 30, NEX: 1) sequences.

Preprocessing of diffusion-weighted images

The FMRI Software Library of FSL (www.fmrib.ox.ac.uk/fsl) was used for analyzing diffusion-weighted images for each subject.

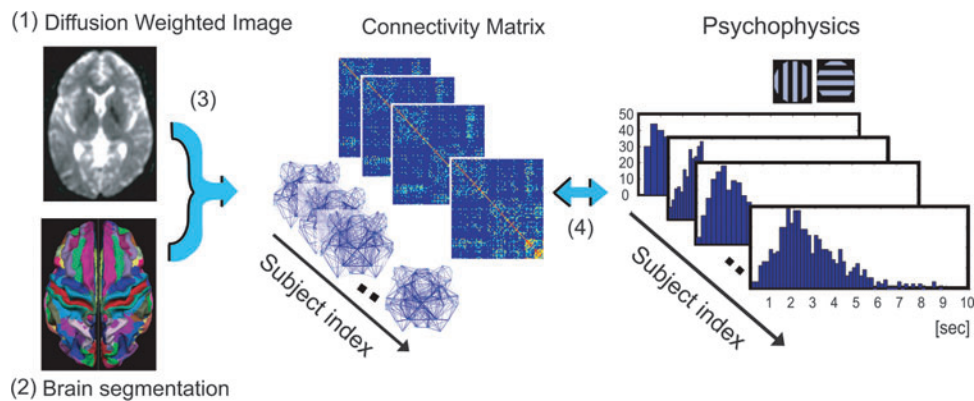


FIG. 1. Scheme of data analysis. (1) The segmentation map on T1-weighted images was calculated for individual participants. (2) After reducing the noise of diffusion-weighted images, fractional anisotropy (FA) values were calculated for individual participants. (3) Segmentation maps were coregistered onto the DWI maps, and fibers were tracked from the FA maps according to the segmentation map. We then developed the association (connectivity) matrix between all pairs of brain regions. (4) Finally, individual participants' differences of the connectivity matrix were compared with the individual participants' differences of results of psychophysical measurements.

All images were corrected for eddy current distortions and head motion specifically by aligning all volumes to the first b0 image. Their diffusion tensors were fitted independently to each voxel in the corrected image, and were used to calculate the FA maps (Basser *et al.*, 1994; Jenkinson and Smith, 2001). The FA value can indirectly quantify the coherence of the orientations of white-matter fiber tracts in the brain (Basser *et al.*, 1994; Le Bihan *et al.*, 2001). High FA values represent more-organized tissues (anisotropic diffusion), and low FA values indicate a lack of directional tissue (isotropic diffusion). In other words, the FA value evaluates the microstructural integrity of white matter tissue (Head *et al.*, 2004; Klingberg *et al.*, 2000; Pfefferbaum *et al.*, 2002). By tracking the principle direction of the diffusion of FA values, we can also reconstruct fiber tracts.

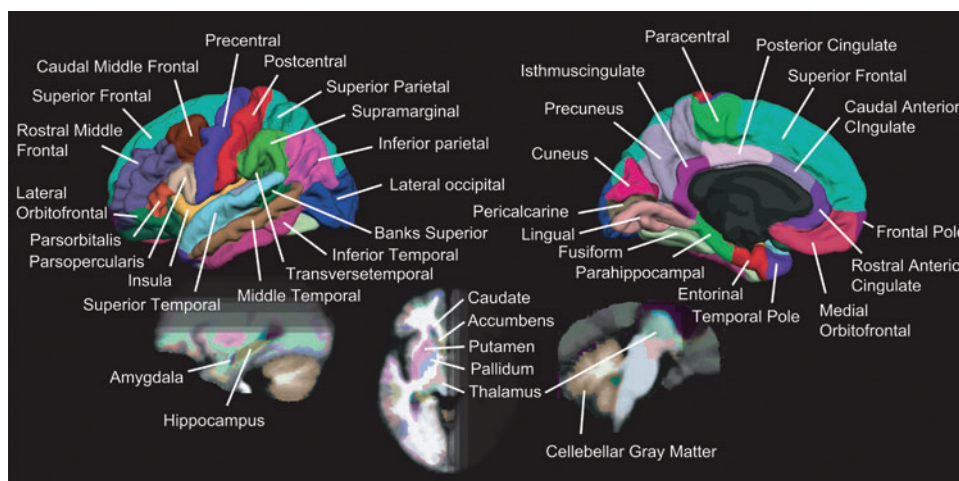
Brain segmentations and nodes of networks

The cortical surface was parcellated by using the template (fsaverage) of FreeSurfer Software (<http://surfer.nmr.mgh.harvard.edu/>) according to the criterion of *aparc+aseg*

.mgz/. The subcortical regions were automatically segmented by analyzing the T1-weighted images of individual participants. Using this approach, we could prepare all 84 regions of interest (ROIs), including 68 cortical ROIs and 16 subcortical ROIs, as shown in Figure 2 (Desikan *et al.*, 2006). The segmentation template is defined by an automated technique, not only to parcellate the cerebral cortex but also to segment the subcortical regions (Fischl, *et al.*, 2002). Although the technique is automatic, the accuracy has been demonstrated to be comparable to manual labeling, which requires several weeks for a trained neuroanatomist or technician to do manually (Fischl *et al.*, 2002, 2004).

T1-weighted images were spatially normalized according to the Montreal Neurological Institute template brain. The resulting normalization parameters were subsequently applied to the individual diffusion-weighted images and FA images for reorienting the gradient directions using SPM8 (www.fil.ion.ucl.ac.uk/spm/software/spm8). Then, we fitted the prepared cortical and subcortical ROIs onto the b0 image in the diffusion-weighted images. We checked all of the overlapping data carefully for both cortical and subcortical ROIs.

FIG. 2. The map of segmented brain regions. The segmentation map includes 68 cortical and 16 subcortical regions of interest (ROIs).



Before calculating the correlation between FA values in ROIs and variables representing psychophysical properties, we changed FA values outside of the brain region to zero.

Fiber tracking and links of networks

FA values can characterize the preferred direction of the white matter running through each voxel (Le Bihan, 2001). Based on this calculation, we reconstructed white-matter fiber tracts using the FACT fiber-tracking algorithm between each pair of ROIs (Mori and Barker, 1999; Mori and van Zijl, 2002; Xue *et al.*, 1999) by using Camino software (<http://cmic.cs.ucl.ac.uk/camino/>). The seed point of each ROI was selected at the gravity center of all voxels included in each ROI. In the tracking between two seeds, if the curvature of streamline exceeded 40° at each step, we rejected the streamline.

From the reconstructed fiber-tract bundle, we created connectivity matrices for each individual participant. In the connectivity matrices, we regarded one pair of nodes as being connected if there was at least one streamline, and we defined weighed factors of each connection using each mean FA value in voxels constituting each fiber-tract bundle connecting between two regions. Then, we excluded the voxels included in ROIs, which were used as edges of these networks.

Psychophysical experiments

The psychophysical experiment on each day consisted of four 15-min sessions (Fig. 3). During each session, participants viewed stimuli consisting of a superimposed vertical and horizontal grating (2.66 cycle/deg) within a circle region (3.0° diameter) around a fixation cross (two perpendicular lines, each 0.4° long and 0.2° wide) through stereoscopic glasses that caused the binocular rivalry phenomenon. The contrast of all gratings was 20%, and their average luminance

was 23.5 cd/m². The color of either vertical or horizontal visual-grating stimulus was red, and the opposite was green. Stereoscopic glasses were green and red (Fig. 3). The filters of the stereoscopic glasses transmitted <3% of the unmatched versus matched luminance color (Tong, *et al.*, 1998). Therefore, each of the participant’s eyes received only one of the vertical and horizontal grating information at a time. The participants were instructed to maintain steady fixation, and to press one of two keys corresponding to one of the two perceptions as soon as the dominantly perceived direction of gratings changed. The relationship between perceptions and finger indications were counterbalanced among the participants. The participants were also instructed not to control perception intentionally and to view stimuli passively.

As shown in Figure 3, the green and red lenses of the stereoscopic glasses were exchanged after 2nd session and the colors of the vertical and the horizontal grating were exchanged at the end of 1st and 3rd sessions to counterbalance the biases toward certain colors of glasses in the preferred eye of the participants. All visual stimuli were projected on a translucent screen (visual angle of 30°×40°) using a digital processing light projector, and were generated using the psychophysics toolbox in MatLab (Brainard, 1997). The participants’ eye movements were carefully monitored during the experiment using a SensoMotoric Instruments Eyelink System (Teltow, Germany). In the evaluation of psychophysical results, we used speeds of perceptual alternation, which were defined as the inverse of the mean value of duration of the time length of perceptual alternations (histogram at right side of Fig. 1). The definition was used here because

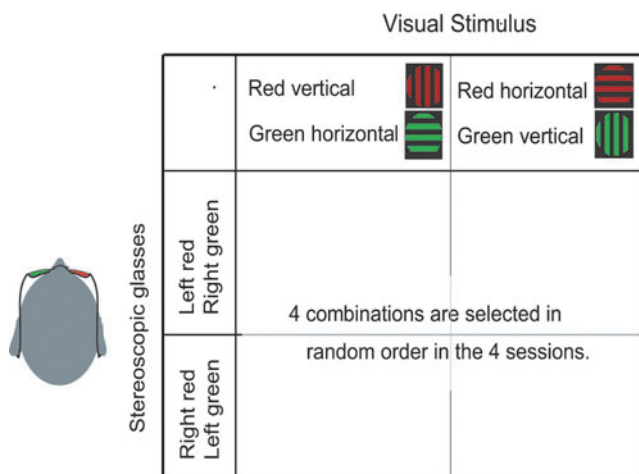


FIG. 3. Design of the binocular rivalry experiment. Only red grating is visible by one eye through a green filter, and only green grating is visible by the other eye through a red filter. Across the first two sessions, the red stimulus was a horizontal grating, and the green stimulus was a vertical grating. In the remaining two sessions, the colors of two directions of grating were exchanged, and within each pair of sessions, the colors of filters were exchanged. Participants experienced these four kinds of combinations of visual stimuli and visual filters in a random order within 1 day.

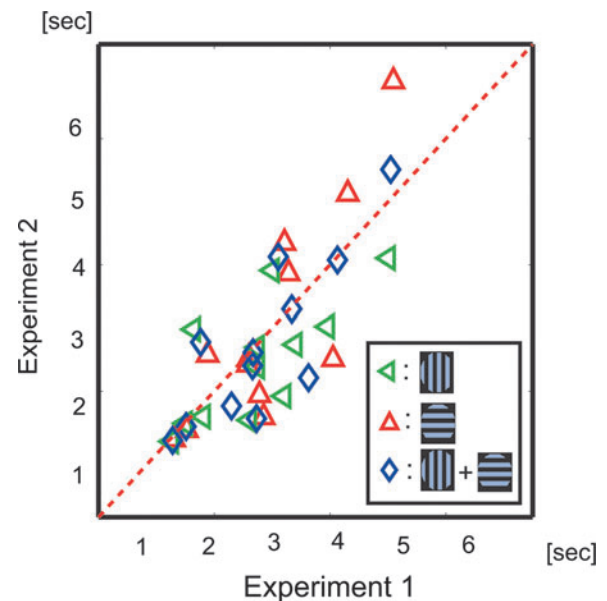


FIG. 4. Stability of alternation speed of perceptual switching. Twelve of the 17 participants completed both phases of the psychophysical experiment. The interval between the two experiments was longer than 3 weeks. Green triangles indicate the average duration in time of vertical grating perception; red triangles indicate the average duration in time of horizontal grating perception; and blue indicates the average duration in time of all perceptual alternations. The correlation between the two experiments was 0.71 ($p < 0.01$).

the parameter showed a significant stability between two psychophysical experiments within each participant (Fig. 4; Aafjes *et al.*, 1966; George, 1936; McDougall, 1906).

Comparison between perceptual properties and corresponding brain structures

To compare between the brain structures and psychophysical properties, we calculated the correlation between the differences among the mean FA values in individuals' brain structures and the differences among individuals' speeds of perceptual alternation. After fiber tracking, we compared the mean FA values in all voxels consisting fiber-tract bundles with the psychophysical parameter. We used nonparametric

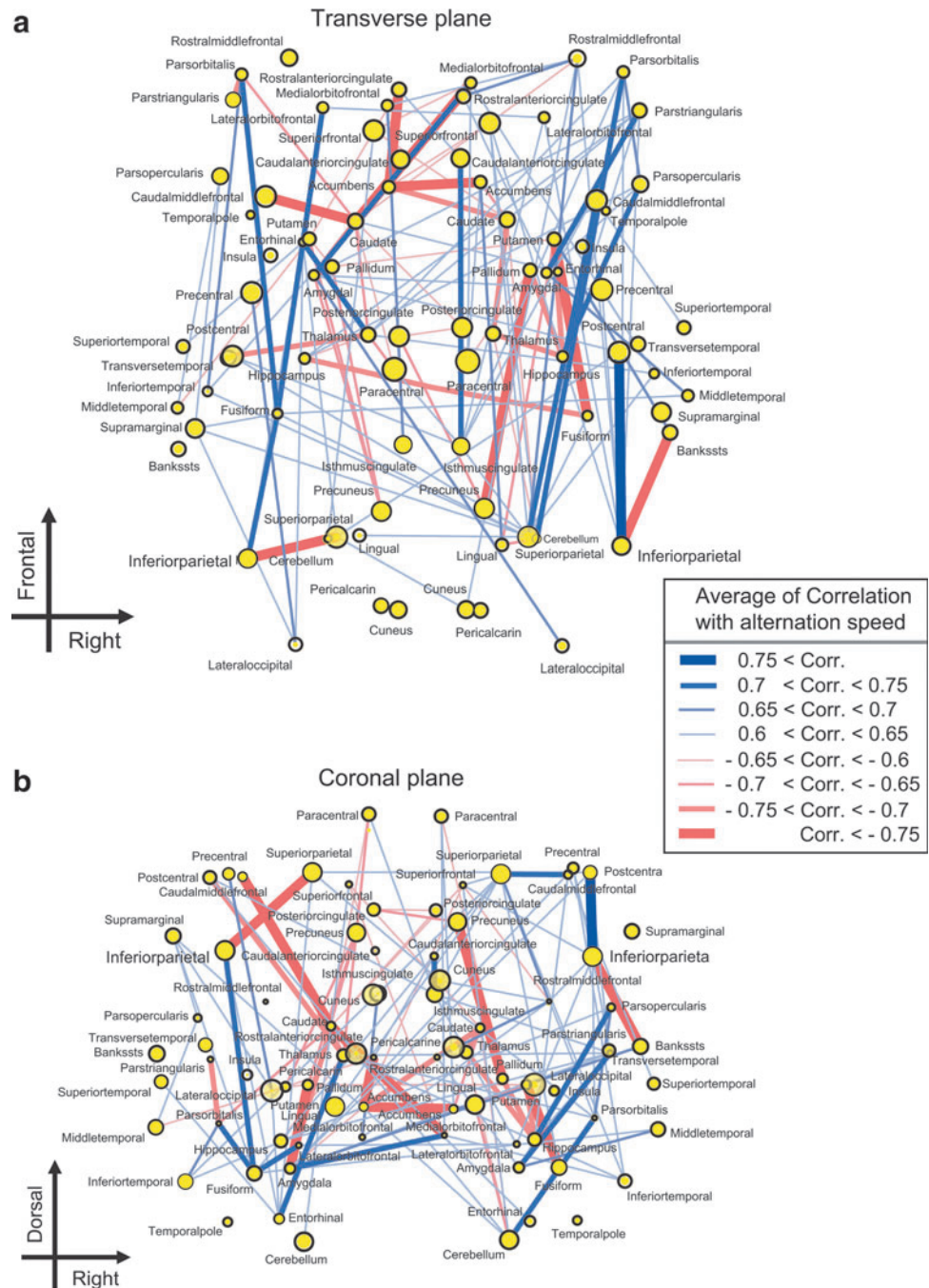
Spearman's rank tests of the correlation coefficients between the averaged FA values in each fiber-tract bundle using MatLab. The fiber-tract bundle, in which averaged FA value showed positive correlation with the speed of perceptual alternation, was referred to as positive correlation networks (CNs), and the fiber-tract bundle, in which the averaged FA value showed negative correlation with the speed of perceptual alternation, was referred to as negative CNs.

Results

Stability in psychophysical measures

In the psychophysical experiment, we recorded the time sequence of the perceptual alternation between vertical and

FIG. 5. Positive and negative correlation networks (CNs). Correlations between the averaged FA values among voxels included in the tracts and speed of perceptual alternation are shown here. (a) and (b) demonstrate the spatial mapping on the transverse plane and on coronal plane, respectively. The blue lines show positive CNs (bundles of tracts showing positive correlation with the speed of perceptual alternations), and the red links show negative CNs (bundles of tracts showing negative correlation with speed of perceptual alternations). The size of yellow dots indicates the depth of the brain regions in the three-dimensional space. When the intensity of correlation value is 0.7, the corresponding *p*-value in Spearman's rank test is ~ 0.01 , and the expected value of false discovery rate (FDR) is < 0.05 (Benjamini and Hochberg, 1995).



horizontal gratings. Figure 4 shows the comparison between the mean values of duration of the time lengths of the two experiments. The two experiments were separated by a space of longer than 3 weeks. Comparing these two experiments, the results clearly demonstrate significant stability for each individual participant ($R = 0.71, p < 0.01, t$ -test).

Perceptual bias and network architecture

To observe the interaction among various brain regions, we mapped the structural network architecture of the whole human brain. In Figure 5, each line indicates a bundle of fiber tracts connected to a pair of brain regions. The color of the line indicates signs (blue lines are positive CNs and red lines are negative CNs) of correlations among each averaged FA value of each fiber tract and each participants' speed of perceptual alternation. Thick lines represent significantly strong connections; a correlation value of 0.7 corresponds with a p -value 0.01 in Spearman's rank test, and the corresponding expected value of false discovery rate (FDR) is < 0.05 (Benjamini and Hochberg, 1995). Therefore, for this threshold, multiple comparisons were sufficiently avoided by using FDR.

This result showed that these two types of fiber-tract bundles were entangled each other. To understand the topological organization by disentangling it, we performed the following analysis.

Key properties of positive CNs and negative CNs

We evaluated how the distances of the fiber-tract bundles changed in relation to the correlation changes between individuals' differences of FA values and their differences of speeds of perceptual alternation. In other words, we observed how widely positive CNs and negative CNs distribute (Fig. 6). The distribution of these two types of fiber-tract bundles showed significantly different sizes of distributions: negative CNs were significantly more localized than the positive CNs in both the hemispheres (Fig. 6a, b). Their p -values of 1-sided t -test are shown in Figure 6c and d.

To determine where the localized regions connect with densely distributed negative CNs, we reorganized the spatial mapping of the networks, as shown in Figure 5a. In Figure 7, the y -axis was changed from a spatial location to the total value of correlations between the averages of FA values of the fiber tracts connecting to each brain region and speeds of perceptual alternation. This distribution shows a clear pattern, which is wider at the top and narrower at the bottom. Therefore, many negative CNs are localized around the central region of the brain. However, among brain regions whose averaged correlation was positive (distributing in the upper side of Fig. 7), only connections from the bilateral inferior parietal regions were connected with a strong negative CN. This result suggests that the inferior parietal regions are special regions for competition between acceleration and deceleration of perceptual alternation. This finding is consistent with a previous study based on individual brain regions. In this study, we tried to think more about the important new finding that many negative CNs are localized around the central region of the brain.

Next, we calculated the difference of correlations between FA values and speed of perceptual alternation separately for the cortical regions and for the subcortical regions.

Figure 8a depicts the average of the correlations in fiber-tract bundles connected to each cortical region. Figure 8b

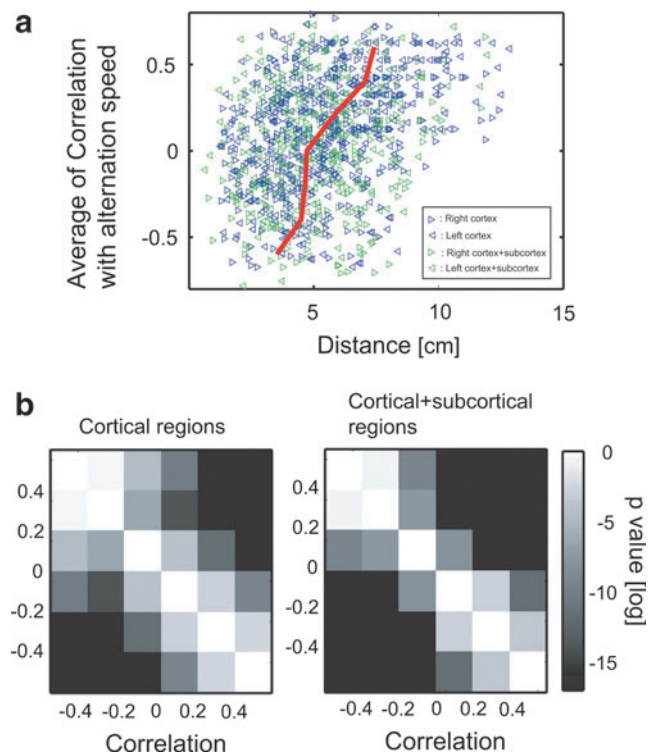


FIG. 6. Localization of negative CNs: Figure (a) shows relationships between the distances between brain regions in the left and right hemispheres (the lengths of tracts as shown in figure 2 and the correlation between FA values in the tracts and their alternation speeds of perceptual switching. Green triangles show results of all cortical and subcortical regions. Blue triangles, which are results only among cortical regions, are overlaid on top of the green triangles. The red line is the fitted line for whole brain data. Figure (b) shows p -values of t -tests about the differences of Euclidian distances between each pair of connected edges depending on the correlations for results shown in the figure (a). Here, the grid size of correlation strength is 0.2. Within figure (b), the left figure is a result of data samples only of cortical regions, and the right figure is a result of data samples of both of cortical and subcortical regions. We could observe significant increases of distances between brain regions depending on the increases of the correlation.

depicts the averaged correlation in fiber-tract bundles connecting with each subcortical region. Figure 8c is the comparison between results of the cortex and the subcortices.

Figure 8d was generated using $(N_{+CN} - N_{-CN}) / N_{all}$, where N_{+CN} is the number of positive CNs; N_{-CN} is the number of negative CNs; and N_{all} is the number of all networks within the cortex. Figure 8e uses the same values in Figure 8d for connections within the subcortex, and Figure 8f depicts the comparison between results of the cortex and of the subcortices. These values represent the ratio of positive CNs to negative CNs for each node within the whole-brain network.

Remarkably, all subcortical regions showed negative values both in the average of the correlations and in the ratio of positive CNs to negative CNs within the network. In contrast, almost all cortical regions showed positive values in both cases. This result demonstrates the general property of

FIG. 7. Reorganization of positive and negative CNs. The x -axis is same as in Figure 6a, but the y -axis was changed to be the averaged value of correlations between mean FA values included in bundle of fiber tracts and alternation speed of perception. Correlations were averaged for all bundles of fiber tracts connecting with each node. The sizes of all yellow circles show the averages of absolute values of correlations.

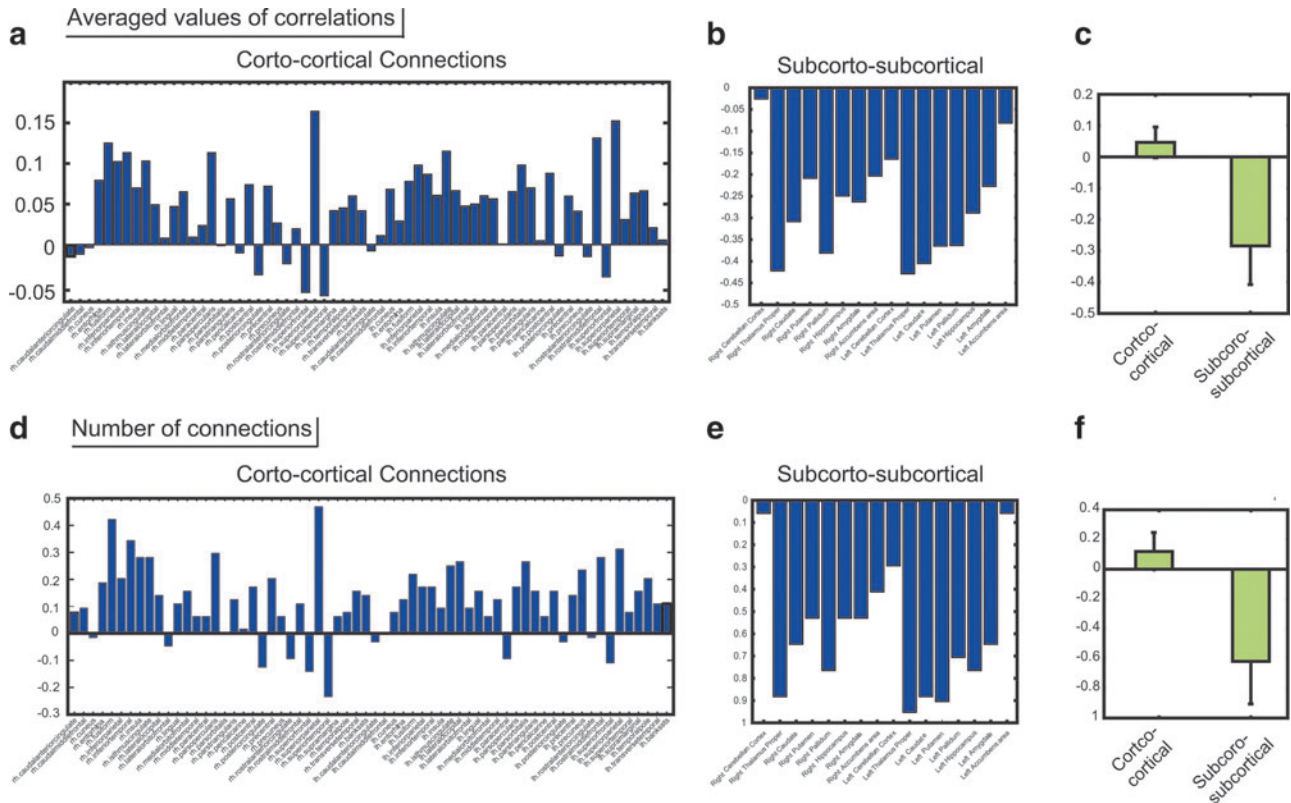
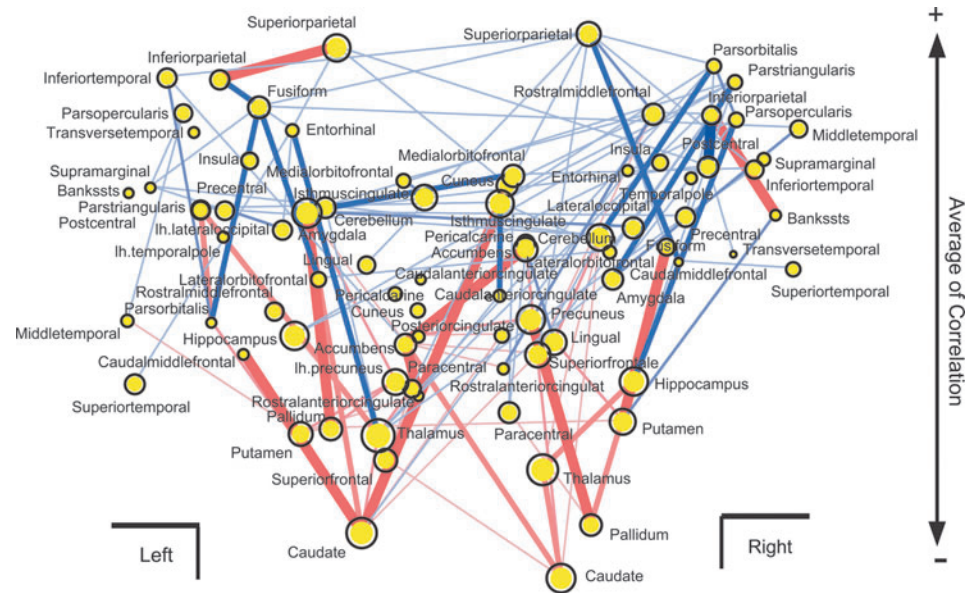


FIG. 8. Comparison between cortical regions and subcortical regions. (a) shows the averaged correlation between FA values included in the bundle of fiber tracts connected with each cortical region and alternation speeds of perceptual switching. The x -axis specifically shows each cortical region, and the y -axis is the averaged correlations. (b) shows the same observation of averaged correlations for the subcortical regions. The two bars in (c) show averages of correlations among all cortical regions shown in (a) among all subcortical regions shown in (b). Stable negative correlations in subcortical regions were observed. (d) shows $(N_{+CN} - N_{-CN}) / N_{all}$, where N_{+CN} is the number of positive CNs; N_{-CN} is the number of negative CNs; and N_{all} is the number of all networks within cortical regions. (e) shows the same variable for the networks within subcortical regions, and (f) is the comparison between the cortex and subcortices.

the network, where all subcortical regions often strongly connect with negative CNs, and many cortical regions often strongly connect with positive CNs.

In addition, we determined if the significant correlation between the FA values and stabilities of perceptual alternations is caused by the overlapping of the fiber-tract bundles. One possible result is that correlations for two fiber-tract bundles should be closer when the number of overlapped voxels is larger. To evaluate how much more often two fibers are overlapped than an occasional case, we used the overlap index. The overlap index evaluates how much more often two fibers are overlapped than in the occasional case:

$$Overlap\ Index = \frac{N_{overlap}/N}{(N_{tract1}/N)(N_{tract2}/N)}$$

Here, N_{tract1} indicates number of voxels of a fiber-tract bundle (tract 1); N_{tract2} indicates number of voxels of another fiber-tract bundle (tract 2); $N_{overlap}$ indicates number of voxels of overlapped regions of two fiber-tract bundles, N indicates total number of voxels of the whole brain; and N_{tract1}/N or N_{tract2}/N indicates the probability that voxels are included in tract 1 or tract 2 occasionally, and N_{tract1}/N also indicates the probability that overlaps really occurred, as $(N_{tract1}/N)(N_{tract2}/N)$ indicates the probability that an occasional overlap happens when voxels for tract 1 and tract 2 were selected randomly. The overlap index evaluates how much more often two fibers are overlapped than in the occasional case.

Figure 9 shows the contour map of the overlap index between two fiber-tract bundles. If the similarity of correlations between two fiber-tract bundles is caused by overlaps between two fibers, the white regions indicating a high overlap index may congregate around the diagonal line. However, the actual results showed no clear bias to diagonal components.

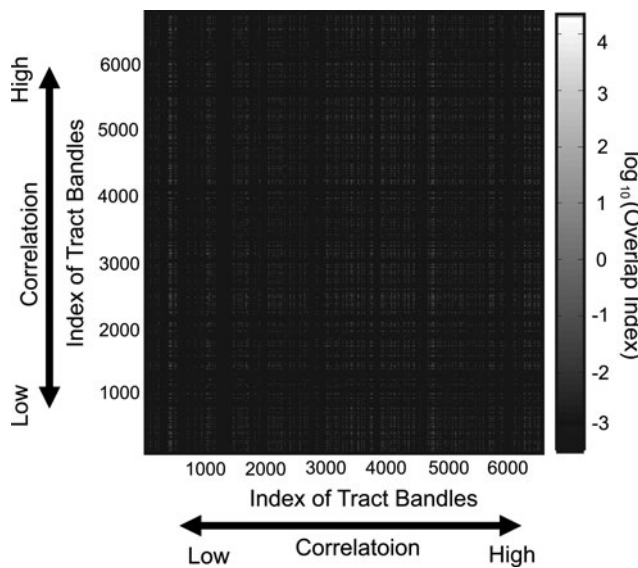


FIG. 9. Color map of the overlap index between two fiber-tract bundles. The x - and y -axes correspond with correlations between the FA values of these two fiber-tract bundles and the stability of perceptual alternation. If the overlap is causing the artificial correlations, then the overlap index would be high around the diagonal regions.

Discussion

Summary of main findings

In this study, we asked how the structural brain network relates to the perceptual alternation in binocular rivalry. Three new trends of spatial mapping of the global architecture of the whole-brain structural network were revealed from evaluation of positive or negative correlations between averaged FA values on fiber tracts connecting between 84 brain structures and speeds of perceptual alternations. First, all averaged FA values of networks connecting between the subcortical regions showed stable negative correlations with alternation speed. Second, networks within almost all cortical regions showed positive correlations. Third, almost all other fiber-tract bundles showing negative correlation belonged to one central cluster of networks within the subcortical networks (Fig. 7). In the following subsections, we discuss the relationship of these findings to the global organization of the whole-brain structural network.

Cortical regions

In previous studies, the importance of the prefrontal and parietal regions in stabilization and acceleration of perceptual alternation has been reported (Kanai *et al.*, 2010a; Sterzer and Kleischmidt, 2007; Windmann *et al.*, 2006). Our study showed a significant correlation of connections between the prefrontal cortex and parietal cortex in relation to the speed of perceptual alternation. In the left hemisphere, the medial orbital cortex was found to be connected to the inferior parietal cortex through a strong negatively correlated network, and in the right hemisphere, the caudal medial frontal cortex was found to be connected with to the superior parietal cortex. These results suggested that the network can stabilize or destabilize by switching between negative or positive interconnections between the prefrontal cortex and the parietal cortex. In addition to these findings, our research showed that almost all the cortical regions are mainly connected with positive CNs (Fig. 8a, d). Further, we also found that almost all remaining negative CNs, which connected with the cortical regions, created one large cluster of connections with negative CNs that connect within the subcortical regions (Fig. 7).

Only one exception to these results was found in the bilateral inferior parietal regions; although the bilateral inferior parietal regions mainly connect with positive CNs, they also connect with strong negative CNs. (Fig. 7). These results are supported by previous findings from a region-based study (Kanai *et al.*, 2010b). Although our network approach is new for visual perception, this network-based approach can detect the findings consistent with classical region-based analyses. The negative CNs of the inferior parietal regions did not connect with the big cluster of negative CNs that mainly consisted of the subcortical regions. This new finding suggests that the inferior parietal regions may be a locus within the cortex responsible for conflicts between bias toward stabilization and bias toward destabilization of perceptual alternation.

Subcortical regions

As demonstrated in 4.1., the subcortical regions are mainly connected with negative CNs. Within the global organization in the subcortical networks relating to stabilization, the

thalamus connected most frequently with negative CNs and showed the largest negative averaged value of correlations (Fig. 8b, e). In previous studies, the importance of the thalamus in perceptual alternation has been reported (Haynes *et al.*, 2005; Shimono, *et al.*, 2011b; Winderlich, *et al.*, 2005); however, high negative correlations and a high rate of connection with negative CNs were also found in the caudate, putamen, and pallidum etc. (Fig. 8b, e). All of these brain regions connect with each other as one large cluster (Fig. 7). Future studies may provide new opportunities for a deeper understanding of whole information processing of the perceptual alternation phenomenon through interconnections between these various subcortical regions.

Further evaluation of DTI

In Figure 9, we show how the number of overlaps existing between two fiber tracts influences their correlations. If the overlaps caused similarities of correlations between two fiber-tract bundles, then a high overlap index should be observed around the diagonal regions. However, the densities of overlaps at nondiagonal regions were similar to the densities around the diagonal regions. Therefore, the significant correlations between FA values and stability of perceptual alternations were caused by overlaps between fiber-tract bundles. The mean diffusivity (MD) values were also evaluated using the same method used in this report. However, the MD did not show stable results between the two separated experiments performed on each of the individual participants (data not shown).

Although FA values are often used to represent the information transmission efficiency or integrity of white-matter fibers, it is not completely understood what the FA value physiologically represents, because the FA value is influenced by many physiological factors, such as myelination, axon diameter, axon density, and ultrastructure (Beaulieu, 2002).

Remarks and perspectives

This study revealed, for the first time, the global organization of the brain networks relating to stabilization and destabilization of perceptual alternation. An understanding of the general contrast between the contribution of the cortical regions to destabilization and the contribution of the subcortical regions to stabilization of perceptual alternation will lead to a clearer understanding of interactions of many local brain regions. The approach of directly treating the global organization of the networks interconnecting various parts of the brain will be effective in understanding the complex organization of the brain related to various cognitive tasks.

Acknowledgments

M.S. is grateful to Olaf Sporns for important comments on this document, Ryusuke Hayashi to his fruitful discussion, Daich Nozaki for his many supports to accomplish this research, and Doris Zakian for fruitful comments in writing this document. This research was supported by Grants-in-Aid for JSPS fellow to M.S. and Grants-in-Aid for Scientific Research (20240026) to K.N.

Author Disclosure Statement

No competing financial interests exist.

References

- Aafjes M, Hueting JE, Visser P. 1966. Individual and interindividual differences in binocular retinal rivalry in man. *Psychophysiology* 3:18–22.
- Basser PJ, Mattiello J, LeBihan D. 1994. Estimation of the effective self-diffusion tensor from the NMR spin echo. *J Magn Reson B* 103:247–254.
- Benjamini Y, Hochberg Y. 1995. Controlling the false discovery rate: a practical and powerful approach to multiple testing. *J R Statist Soc B* 57:289–300.
- Blake R. 1989. A neural theory of binocular rivalry. *Psychol Rev* 9:145–167.
- Blake R, Logothetis NK. 2002. Visual competition. *Nat Rev Neurosci* 3:4–11.
- Brainard DH. 1997. The psychophysics toolbox. *Spat Vis* 10:433–436.
- Beaulieu C. 2002. The basis of anisotropic water diffusion in the nervous system - a technical review. *NMR Biomed* 15: 435–455.
- Bullmore E, Sporns O. 2009. Complex brain networks: graph theoretical analysis of structural and functional systems. *Nat Rev Neurosci* 10:186–198.
- Crick F, Koch C. 1998. Consciousness and neuroscience. *Cereb Cortex* 8:97–107.
- Desikan RS, Segonne F, Fischel B, Quinn BT, Dickerson BC, Blacker D, Buckner RL, Dale AM, Maguire RP, Hyman BT, Albert MS, Killiany RJ. 2006. An automated labeling systems for subdividing the human cerebral cortex on MRI scans into gyral based regions of interest. *NeuroImage* 31:968–980.
- Doesburg SM, Green JJ, McDonald JJ, Ward LM. 2009. Rhythms of consciousness: binocular rivalry reveals large-scale oscillatory network dynamics mediating visual perception. *PLoS One* 4:e6142.
- Doesburg SM, Kitajo K, Ward LM. 2005. Increased gamma-band synchrony precedes switching of conscious perceptual objects in binocular rivalry. *Neuroreport* 16:1139–1142.
- Felleman DJ, Van Essen DC. 1991. Distributed hierarchical processing in primate cerebral cortex. *Cereb Cortex* 1:1–47.
- Fischl B, Salat DH, Busa E, Albert M, Dieterich M, Haselgrove C, van der Kouwe A, Killiany R, Kennedy D, Klaveness S, Montillo A, Makris N, Rosen B, Dale AM. 2002. Whole brain segmentation: automated labeling of neuroanatomical structures in the human brain. *Neuron* 33:341–355.
- Fischl B, van der Kouwe A, Destrieux C, Halgren E, Segonne F, Salat D, Busa E, Seidman L, Goldstein J, Kennedy D, Caviness V, Makris N, Rosen B, Dale AM. 2004. Automatically parcellating the human cerebral cortex. *Cereb Cortex* 14:11–22.
- George RW. 1936. The significance of the fluctuations experienced in observing ambiguous figures and in binocular rivalry. *J Gen Psychol* 15:39–61.
- Grossberg S. 1987. Cortical dynamics of three-dimensional form, color and brightness perception: 2. Binocular theory. *Percept Psychophys* 41:117–158.
- Hagmann P, Cammoun L, Gigandet X, Meuli R, Honey CJ, Wedeen VJ, Sporns O. 2008. Mapping the structural core of human cerebral cortex. *PLoS Biol* 6:e159.
- Hagmann P, Kurant M, Gigandet X, Thiran P, Wedeen VJ, Meuli R, Thiran J-P. 2007. Mapping human whole-brain structural networks with diffusion MRI. *PLoS One* 2:e597.
- Hänggi J, Wotruba D, Jäncke L. 2011. Globally altered structural brain network topology in grapheme-color synesthesia. *J Neurosci* 31:5816–5828.
- Haynes JD, Deichmann R, Rees G. 2005. Eye-specific effects of binocular rivalry in the human lateral geniculate nucleus. *Nature* 438:496–499.

- Head D, Buckner RL, Shimony JS, Williams LE, Akbudak E, Conturo TE, McAvoy M, Morris JC, Snyder AZ. 2004. Differential vulnerability of anterior white matter in nondemented aging with minimal acceleration in dementia of the Alzheimer type: evidence from diffusion tensor imaging. *Cereb Cortex* 14:410–423.
- Hipp FJ, Engel KA, Siegel M. 2011. Oscillatory synchronization in large-scale cortical networks predicts perception. *Neuron* 69:387–396.
- Hock H S, Schonher G, Voss A. 1997. The influence of adaptation and stochastic fluctuations on spontaneous perceptual changes for bistable stimuli. *Percept Psychophys* 59:509–522.
- Jenkinson M, Smith S. 2001. A global optimisation method for robust affine registration. *Med Image Anal* 5:143–156.
- Kanai R, Bahrami B, Rees G. 2010a. Human parietal cortex structure predicts individual differences in perceptual rivalry. *Curr Biol* 20:1626–1630.
- Kanai R, Carmel D, Bahrami B, Rees G. 2010b. Structural and functional fractionation of right superior parietal cortex in bistable perception. *Curr Biol* 21:R106–R107.
- Kleinschmidt A, Buchel C, Zeki S, Frackowiak RS. 1998. Human brain activity during spontaneously reversing perception of ambiguous figures. *Proc Biol Sci* 265:2427–2433.
- Klingberg T, Hedehus M, Temple E, Salz T, Gabrieli JD, Moseley ME, Poldrack RA. 2000. Microstructure of temporo-parietal white matter as a basis for reading ability: evidence from diffusion tensor magnetic resonance imaging. *Neuron* 25:493–500.
- Knapen T, Brascamp J, Pearson J, van Ee R, Blake R. 2011. The role of frontal and parietal brain areas in bistable perception. *J Neurosci* 31:10293–10301.
- Kohler W, Wallach H. 1944. Figural after-effects: an investigation of visual processes. *Proc Am Philos Soc* 88:269–357.
- Kovacs I, Parathomas TV, Yang MF, Feher A. 1996. When the brain changes its mind: Interocular grouping during binocular rivalry. *Proc Natl Acad Sci* 93:15508–15511.
- Le Bihan D, Mangin JF, Poupon C, Clark CA, Pappata S, Molko N, Chabriat H. 2001. Diffusion tensor imaging: concepts and applications. *J Magn Reson Imaging* 13:534–546.
- Lee S-H, Blake R. 1999. Rival ideas about binocular rivalry. *Vis Res* 39:1447–1454.
- Lee S-H, Blake R. 2004. A fresh look at interocular grouping during binocular rivalry. *Vis Res* 44:983–991.
- Lee S-H, Blake R, Heeger DJ. 2007. Hierarchy of cortical responses underlying binocular rivalry. 10:1048–1054.
- Lehky SR. 1988. An astable multivibrator model of binocular rivalry. *Perception* 17:215–228.
- Leopold DA, Logothetis NK. 1996. Activity changes in early visual cortex reflect monkeys' percepts during binocular rivalry. *Nature* 379:549–553.
- Levelt W. 1965. *On Binocular Rivalry*. Soesterberg, The Netherlands: Institute for Perception RVO-TNO.
- Logothetis NK, Leopold DA, Sheinberg DL. 1996. What is rivaling during binocular rivalry? *Nature* 28:621–623.
- Logothetis N, Schall J. 1989. Neuronal correlates of subjective visual perception. *Science* 245:761–763.
- Lumer ED, Friston KJ, Rees G. 1998. Neural correlates of perceptual rivalry in the human brain. *Science* 280:1930–1934.
- Lynall ME, Bassett DS, Kerwin R, McKenna PJ, Kitzbichler M, Muller U, Bullmore E. 2010. Functional connectivity and brain networks in schizophrenia *J Neurosci* 30:9477–9487.
- Matsuoka K. 1984. The dynamic model of binocular rivalry. *Biol Cybern* 49:201–208.
- McDougall W. 1906. Physiological factors of the attention-process (IV). *Mind* 15:329–359.
- Mori S, Barker PB. 1999. Diffusion magnetic resonance imaging: its principle and applications. *Anat Rec* 257:102–109.
- Mori S, van Zijl PC. 2002. Fiber tracking: principle and strategies—a technical review. *NMR Biomed* 15:468–480.
- Nguyen VA, Freeman AW, Wenderoth P. 2001. The depth and selectivity of suppression in binocular rivalry. *Percept Psychophys* 63:348–360.
- Ooi TL, He Z J. 1999. Binocular rivalry and visual awareness: the role of attention. *Perception* 28:551–574.
- Pfefferbaum A, Rosenbloom M, Sullivan EV. 2002. Sex differences in the effects of alcohol on brain structure. *Am J Psychiatry* 158:188–197.
- Sherrington CS. 1906. *Integrative Action of the Nervous System*. New Haven, CT: Yale Univ. Press.
- Shimono M, Kitajo K, Takeda T. 2011a. Neuronal processes for intentional control of perceptual switching: a magnetoencephalography study. *Hum Brain Mapp* 32:397–412.
- Shimono M, Mano H, Niki K. 2011b. A brain structural hub of interhemispheric information integration for apparent motion perception. *Cerebral Cortex* 22:337–344.
- Sporns O, Tononi G, Kötter R. 2005. The human connectome: a structural description of the human brain. *PLoS Comput Biol* 1:e42.
- Sterzer P, Kleinschmidt A. 2007. A neural basis for inference in perceptual ambiguity. *Proc Natl Acad Sci U S A* 104:323–328.
- Struber D, Basar-Eroglu C, Hoff E, Stadler M. 2000. Reversal-rate dependent differences in the EEG gamma-band during multistable visual perception. *Int J Psychophys* 38:243–252.
- Sugie N. 1982. Neural models of brightness perception and retinal rivalry in binocular vision. *Biol Cybern* 43:13–21.
- Tong F, Meng M, Blake R. 2006. Neural basis of binocular rivalry. *TREND Cogn Sci* 10:502–511.
- Tong F, Nakayama K, Vaughan JT, Kanwisher N. 1998. Binocular rivalry and visual awareness in human extrastriate cortex. *Neuron* 21:753–759.
- Van Essen DC, Dierker D. 2007. Surface-based and probabilistic atlases of primate cerebral cortex. *Neuron* 56:209–225.
- Varela F, Lachaux J, Rodriguez E, Martinerie J. 2001. The brain web: phase synchronization and large-scale integration. *Nat Rev Neurosci* 2:229–239.
- Wade NJ. 1998. *A Natural History of Vision*. Cambridge, MA: MIT Press.
- Wheatstone C. 1838. Contributions to the Physiology of Vision—Part the First. On some remarkable, and hitherto unobserved, phenomena of binocular vision. *Phil Trans R Soc Lond* 128:371–394.
- Wilson HR, Blake R, Lee SH. 2001. Dynamics of travelling waves in visual perception. *Nature* 412:907–910.
- Windmann S, Wehrmann M, Calabrese P, Güntürkün O. 2006. Role of prefrontal cortex in attentional control over bistable vision. *J Cogn Neurosci* 18:456–471.
- Wunderlich K, Schneider KA, Kastner S. 2005. Neural correlates of binocular rivalry in the human lateral geniculate nucleus. *Nat Neurosci* 8:1595–1602.
- Xue R, van Zijl PC, Crain BJ, Solaiyappan M, Mori S. 1999. *In vivo* three dimensional reconstruction of rat brain axonal projections by diffusion tensor imaging. *Magn Reson Med* 42:1123–1127.

Address correspondence to:
 Masanori Shimono
 Department of Physics
 Indiana University
 Swain Hall West
 727 E. 3rd Street
 Bloomington, IN 47405-7105
 E-mail: nori417@gmail.com